Available online at www.sciencedirect.com
ScienceDirect
Journal of Molecular Catalysis A: Chemical 270 (2007) 257–263
JOURNAL OF MOLECULAR CATALYSIS A: CHEMICAL
www.elsevier.com/locate/molcata

Selective oxidation of methanol over supported vanadium oxide catalysts as studied by solid-state NMR spectroscopy

Danlin Zeng, Hanjun Fang, Anmin Zheng, Jun Xu, Lei Chen, Jun Yang, Jiqing Wang, Chaohui Ye, Feng Deng *

State Key Laboratory of Magnetic Resonance and Atomic and Molecular Physics, Wuhan Institute of Physics and Mathematics, Chinese Academy of Sciences, Wuhan 430071, PR China

Received 27 November 2006; received in revised form 5 February 2007; accepted 12 February 2007
Available online 16 February 2007

Abstract

Methanol catalytic oxidation over VO_x/Al_2O_3, VO_x/ZrO_2 and VO_x/MgO catalysts has been studied by solid-state nuclear magnetic resonance (NMR) spectroscopy. It was found that stronger acid sites in VO_x/Al_2O_3 result in almost the same selectivities for dimethoxymethane, paraformaldehyde and formic acid, and weaker acid sites in VO_x/ZrO_2 favor the formation of paraformaldehyde, while the VO_x/MgO catalyst with the base support shows high selectivity for formate. Supporting VO_x species on γ-Al_2O_3 and ZrO_2 leads to the formation of Brønsted acid sites as revealed by the adsorption of probe molecules. The acid strength of Brønsted acid sites on the VO_x/Al_2O_3 catalyst is found to be stronger than that of the VO_x/ZrO_2 catalyst which has the acid strength similar to zeolite HZSM-5's. The proposed bridging hydroxyl models accounting for the Brønsted acid sites formation were also confirmed by quantum chemical calculation.

Keywords: Methanol oxidation; Vanadium oxide; Solid-state NMR

1. Introduction

Supported vanadium oxide catalysts are extensively used for the selective oxidation of methanol [1–8]. The structures and activities of these catalysts have been widely investigated in the past decades [9–18]. Among them, significant attentions were given to the studies of oxidation of methanol by the VO_x/Al_2O_3, VO_x/ZrO_2 and VO_x/MgO catalysts. However, most of the works have focused only on the nature of surface vanadium species. Isaguliants and Belomestmykh [17] suggested that the formation of pyrovanadate species ($Mg_2V_2O_7$) in VO_x/MgO makes the catalyst efficient for methanol oxidation, while Bars et al. [18] reported that vanadate dimmers are the active sites for oxidation dehydrogenation. Generally, in addition to the vanadium species, the support also plays a crucial role during the methanol oxidation reaction. Unfortunately, the acidic nature of these catalysts and their influence on the product distribution remain unknown. Solid-state nuclear magnetic resonance (NMR) is a well-established technique to trap the intermediates in the heterogeneous reaction and reveal structures of catalysts [19–23]. With the application of the probe molecules, it is successfully applied in characterizing the acidity of various solid acid catalysts [24–33]. Theoretical calculation can reveal the acid strength, interactions between probe molecule and acid sites as well as the reaction transition state formed on zeolites [34–37]. Haw and co-workers [36–39] calculated proton affinity (PA) and ^{13}C chemical shift of adsorbed 2-^{13}C-acetone in order to measure the acidic strength of various solid acids. Our previous studies [40] also demonstrated that theoretical calculation is an efficient method to predict ^{13}C chemical shifts of various organic species adsorbed on zeolites. In this contribution, three supported vanadium catalysts with different acidic properties were prepared by impregnation method. The catalytic oxidation reaction of methanol was investigated in detail by solid-state NMR spectroscopy. Theoretical calculation was employed as well on the models that were proposed based on our NMR experimental results to study the structure and acidity of the catalysts.

* Corresponding author. Tel.: +86 27 8719 8820; fax: +86 27 8719 9291.
E-mail address: dengf@wipm.ac.cn (F. Deng).

1381-1169/$ – see front matter © 2007 Elsevier B.V. All rights reserved.
doi:10.1016/j.molcata.2007.02.009

2. Experimental

2.1. Sample preparation

Vanadium was introduced onto γ-Al_2O_3 (Merk), MgO (Merk) and $ZrO(OH)_2$ [41] by wetness impregnation with an aqueous NH_4VO_3 solution. After impregnation, the materials were dried at 393 K for 5 h and then calcined at 773 K for 12 h in air. The physical characteristics of the catalysts are listed in Table 1. The calcined sample was placed into a glass ampoule and activated at 673 K under vacuum (10^{-3} Pa) for 5 h. 1 mmol methanol (^{13}C, 99%, Cambridge Isotope Inc.) and 0.5 mmol O_2/g catalyst were adsorbed in the ampoule under vacuum at the temperature of liquid nitrogen and then the ampoule was flame sealed. Prior to NMR measurements, the sealed ampoule was warmed to room temperature, heated at the desirable temperature for 15 min and then the reaction was quickly quenched by liquid nitrogen. For the adsorption of probe molecules, samples were kept at 673 K under the vacuum at less than 1×10^{-3} Pa for at least 8 h. To minimize the possible chemical exchange and polymerization, the adsorption of 2-^{13}C-acetone was done at room temperature with a loading of *ca.* 0.1 mmol/g catalyst. The adsorption procedure of trimethylphosphine oxide (TMPO) was different from that of 2-^{13}C-acetone. About 0.5 g dehydrated sample was mixed with 3 ml CH_2Cl_2 solution containing 0.1 M TMPO in a glovebox before the mixture was stirred for 3 h by an ultrasonic shaker, allowed to equilibrate for 5 h and then evacuated under vacuum to remove CH_2Cl_2 completely before NMR measurements.

2.2. Sample characterization

All the NMR experiments were carried out at 9.4 T on a Varian Infinityplus-400 spectrometer with resonance frequencies of 400.12, 100.4 and 161.9 MHz for ^1H, ^{13}C and ^{31}P, respectively. The 90° pulse widths for ^1H, ^{13}C and ^{31}P were measured to be 3.7, 4.4 and 3.6 μs, respectively. The chemical shifts were referenced to tetramethylsilane (TMS) for ^1H, to hexamethylbenzene (HMB) for ^{13}C and to 85% H_3PO_4 solution for ^{31}P, respectively. Repetition times of 6 s for ^1H and 60 s for ^{31}P single-pulse experiments were used. The magic-angle spinning (MAS) rate was 5 kHz. Single pulse ^{13}C MAS NMR spectra were recorded with a 10 s recycle delay, allowing a quantitative measurement of the ^{13}C signals. Cross polarization with interrupted decoupling is also employed for spectral assignments.

Table 1
Vanadium content, surface area for supported VO_x catalysts

Support	Catalyst	V_2O_5 content (wt.%)	BET surface area (S_{BET}, m^2/g)
γ-Al_2O_3	VO_x/Al_2O_3	10	90
ZrO_2	VO_x/ZrO_2	10	140
MgO	VO_x/MgO	10	180

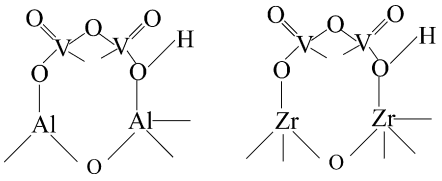

Scheme 1. Possible models of the Brønsted acid sites on the VO_x/Al_2O_3 and VO_x/ZrO_2 catalysts.

2.3. Computational method

The optimizations and chemical shift predictions were carried out using Amsterdam density-functional (ADF) package [42] with the local spin density approximation for exchange and correlation potential employing the Vosko–Wilk–Nusair generalized gradient approximations (GGA) used for the density gradient correction to the exchange and correlation function [43,44]. The triple-zeta basis set including two polarization functions (TZ2P) based on Slater-type orbital (STO) was chosen. 1s–4p orbitals for Zr, 1s–3p orbitals for V and 1s–2p orbitals for Al atoms were kept frozen with the frozen core approximation, while all electron basis sets for the O, C and H atoms are used in the structure optimizations and NMR calculations. It was demonstrated that the relativistic effects are important for V and Zr atoms in defining the geometry of structure; therefore, the calculations were performed within the relativistic scheme with the zero-order regular approximation (ZORA) including the scalar effects [45].

Possible models (Scheme 1) were proposed for the Brønsted acid sites formed on the VO_x/Al_2O_3 and VO_x/ZrO_2 catalysts. No atom in acetone molecule was constrained during all the configuration optimizations of adsorption complexes. The ^{13}C chemical shifts were calculated using the gauge-including atomic orbital (GIAO) method on the optimized structure [46]. The ^{13}C NMR isotropic chemical shift for the carbonyl carbon of acetone adsorption complexes was referenced to the NMR experimental value of the gas-state acetone (208 ppm).

3. Results and discussion

Fig. 1 shows the ^{13}C MAS NMR spectra of methanol and oxygen reaction on VO_x/Al_2O_3 at various temperatures. After adsorption of methanol and oxygen on VO_x/Al_2O_3 at 373 K, four resonances are observable at 49, 53, 69 and 97 ppm. The relatively intense signal at 49 ppm is assigned to methoxyl group [20]. This species cannot be easily removed by vacuum pumping, indicating that it should correspond to surface-bound species. The intensity of this signal gradually decreases as the reaction temperature increase. The signal at 53 ppm is due to the physisorbed methanol [20], which can be easily removed by vacuum pumping. The resonance at 69 ppm is likely due to the ethylene glycol ($HOCH_2CH_2OH$) [47], and the signal at 97 ppm arises from the methylene of dimethoxymethane (DMM) [48]. The appearance of the new signal at 162 ppm (due to formic acid) [49] and a small signal at 90 ppm (due to paraformaldehyde) [20] indicates that methanol has been further oxidized as

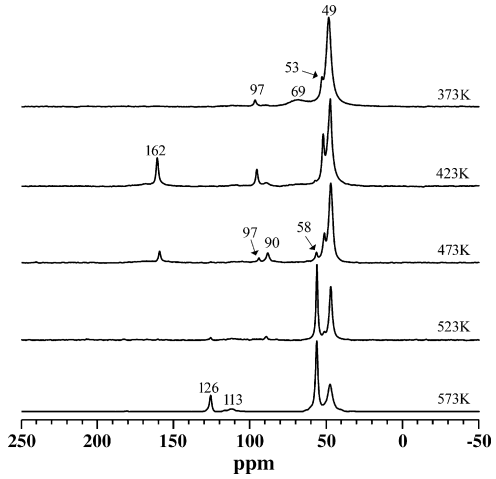

Fig. 1. ^{13}C single-pulse MAS NMR spectra (with proton decoupling) of methanol and oxygen reaction on VO_x/Al_2O_3 at various temperatures.

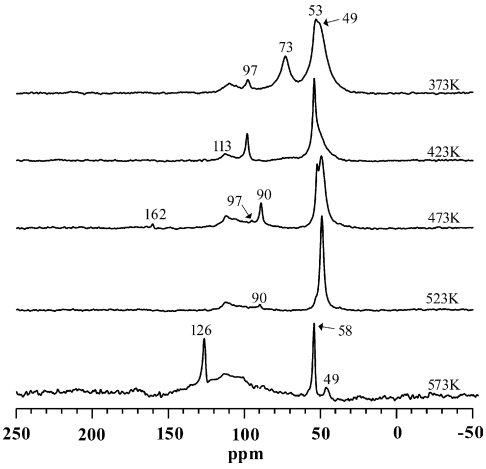

Fig. 2. ^{13}C single-pulse MAS NMR spectra (with proton decoupling) of methanol and oxygen reaction on VO_x/ZrO_2 at various temperatures.

the temperature is elevated to 423 K. When the reaction temperature further increases, the intensity of the 162 and 97 ppm decreases, indicating that high temperature does not favor the formation of formic acid and DMM. We also found that the intensity of the signal at 58 ppm (due to dimethyl ether) [50] increases remarkably as the temperature increases from 423 to 573 K. When the temperature is higher than 523 K, methanol has been oxidized into CO_2 (at 126 ppm) [49]. The resonance at 113 ppm is due to the background of the probe. By careful integration of the various ^{13}C NMR signals (Table 2), we can find that on the VO_x/Al_2O_3 catalyst, the selectivities for DMM (23.2%), paraformaldehyde (30.2%) and formic acid (29.2%) at 473 K are very close.

^{13}C MAS NMR spectra of methanol and oxygen reaction on VO_x/ZrO_2 at various temperatures are shown in Fig. 2. After heating the sample at 373 K for 15 min, the signal at 73 ppm (due to ethylene glycol) appears significantly. The amount of DMM (97 ppm) increases when the temperature is increased from 373 to 423 K. As the reaction temperature increases further from 423 to 473 K, the intensity of paraformaldehyde (90 ppm) increases while the amount of DMM (97 ppm) decreases considerably. A trace of formic acid (162 ppm) is detected at 473 K. As the reaction temperature increases further to 573 K, the signals of formic acid, DMM and paraformaldehyde all disappear and the 126 ppm signal of CO_2 emerges, indicating that some of the hydrocarbons are oxidized into CO_2. Compared with the VO_x/Al_2O_3 and VO_x/MgO catalysts (Table 2), the VO_x/ZrO_2 catalyst seems to display higher selectivity for paraformaldehyde (71.2%) at 473 K.

^{13}C MAS NMR spectra of methanol and oxygen reaction on VO_x/MgO at various temperatures are given in Fig. 3. One dominant resonance at 49 ppm is observed at 423 K, characteristic of methoxyl group. Signals at 62 and 168 ppm (due to dimethyl ether and formate, respectively) are present when the reaction temperature increases to 473 K [51], which is indicative of the occurrence of methanol dehydration to form dimethyl ether and oxidation to form formate. As the reaction temperature increases to 523 K, the intensity of signal at 168 ppm increases and a trace of formic acid (at 162 ppm) is also formed. When the temperature further increases to 673 K, almost all the methanol is oxidized into formate, which suggests that the VO_x/MgO catalyst has higher selectivity for formate compared with the VO_x/Al_2O_3 and VO_x/ZrO_2 catalysts. It is interesting that the signals of dimethoxymethane (DMM) cannot be detected in the VO_x/MgO sample, indicating that Brønsted acid sites play a

Table 2
Methanol oxidation selectivity on supported VO_x catalysts at the same reaction temperature (473 K), the reactant ratio $CH_3OH:O_2 = 2:1$ and reaction time (15 min)

Catalyst	Methanol conversion rate (%)	Selectivity (in C%)		
		DMM	Paraformaldehyde	Formate groups
VO_x/Al_2O_3	21.4	23.3	30.2	29.2 (formic acid)
VO_x/ZrO_2	12.2	20.5	71.2	8.3 (formic acid)
VO_x/MgO	22.4	0	0	79.4 (formate)

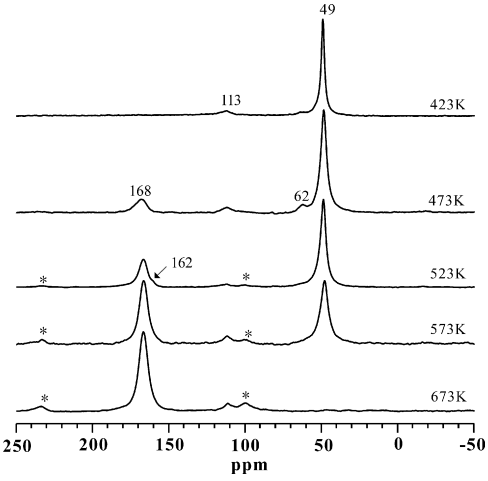

Fig. 3. ^{13}C single-pulse MAS NMR spectra (with proton decoupling) of methanol and oxygen reaction on VO_x/MgO at various temperatures. The asterisks denote spinning sidebands.

crucial role in the formation of dimethoxymethane. The higher selectivity (79.4% at 473 K, Table 2) of the catalyst VO_x/MgO for formate is probably due to the basic property of the MgO support.

In spite of their similar ^{13}C isotropic chemical shifts, formate and carbonate could always be easily distinguished based on their response to interrupted decoupling [20]. The methyl formate signals did not survive interrupted decoupling, as expected for a protonated carbon in a relatively rigid species. On the other hand, signals of carbonate species were not attenuated by interrupted decoupling. In the present case, the intensity of 168 ppm signal decrease significantly in the interrupted decoupling experiment (result not shown), which allows us to assign unambiguously this signal detected in the ^{13}C NMR spectra to formate.

As demonstrated by Haw and co-workers [27,52], 2-^{13}C-acetone can be used as a reliable NMR probe molecule to evaluate the acidic strength of solid acids. The stronger Brønsted acidity will result in stronger hydrogen bonding between the carbonyl carbon and the acidic proton, and consequently, the more downfield of the ^{13}C isotropic chemical shift. Fig. 4 shows the ^{13}C NMR spectrum of 2-^{13}C-acetone adsorbed on VO_x/MgO, VO_x/ZrO_2 and VO_x/Al_2O_3. The signals at 208, 198, 155, 83, 72 and 28 ppm can be assigned to bimolecular, trimolecular and mesityl oxide reaction products of acetone [52]. In Fig. 4a, there is no peak arising from the acetone adsorbed on the Brønsted acid sites, implying the absence of the Brønsted acid sites in the VO_x/MgO catalyst. In the ^{13}C NMR spectrum of 2-^{13}C-acetone adsorbed on VO_x/ZrO_2 (Fig. 4b), two signals (at 223 and 217 ppm) were resolved in the deconvoluted spectrum. The former signal is originated from unreacted acetone adsorbed on the newly formed Brønsted acid sites, while the latter is ascribed to acetone adsorbed on the weakly acidic ZrOH groups present on ZrO_2 [53]. The chemical shift of 223 ppm indicates that acid strength of VO_x/ZrO_2 catalyst is close to that of the bridging OH group in zeolite HZSM-5, where adsorbed 2-^{13}C-acetone gives rise to a ^{13}C resonance at 223 ppm. Similarly, two dominant signals at 217.5 and 225 ppm (due to acetone adsorbed on the weakly acidic AlOH groups and the bridging Brønsted acid sites, respectively) can be observed in the ^{13}C NMR spectrum of acetone adsorbed on VO_x/Al_2O_3 (Fig. 4c). From the ^{13}C acetone NMR results, it can be concluded that the VO_x/Al_2O_3 has an acid strength slightly stronger than the VO_x/ZrO_2 and no Brønsted acid site is present in the VO_x/MgO catalyst.

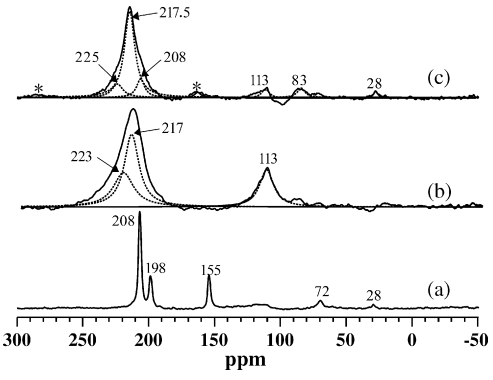

Fig. 4. ^{13}C single-pulse MAS NMR spectra (with proton decoupling) of 2-^{13}C-acetone loaded on (a) VO_x/MgO, (b) VO_x/ZrO_2 and (c) VO_x/Al_2O_3. The asterisk denotes spinning sidebands.

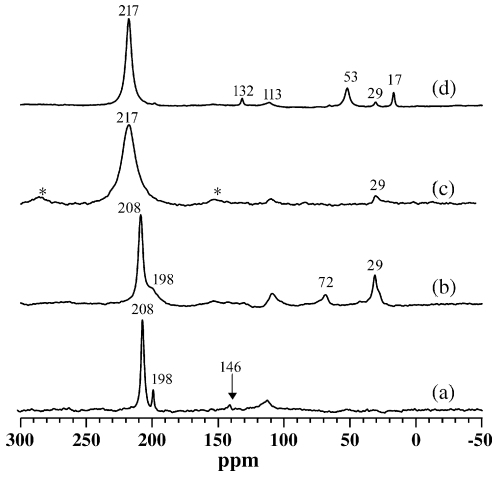

Fig. 5. ^{13}C single-pulse MAS NMR spectrum (with proton decoupling) of 2-^{13}C-acetone loaded on (a) V_2O_5, (b) MgO, (c) ZrO_2 and (d) γ-Al_2O_3. The asterisk denotes spinning sidebands.

We also used 2-^{13}C-acetone as a probe molecule to study the acid sites present on the vanadium oxide (prepared by NH_4VO_3 calcination at 823 K for 5 h), MgO, ZrO_2 and γ-Al_2O_3 (Fig. 5). Besides the peaks associated with diacetone or triacetone alcohol (72 and 29 ppm) and mesityl oxide (208, 198, 146, 132 and 53 ppm) [52], the main ^{13}C signal at 217 ppm can be ascribed to acetone adsorbed on the weakly acidic hydroxyl (ZrOH or AlOH) groups on ZrO_2 and γ-Al_2O_3, indicating the absence of Brønsted acid sites present on these oxides. Obviously, the introduction of vanadium species onto the supports (γ-Al_2O_3, ZrO_2) leads to the formation of new Brønsted acid sites on the VO_x/Al_2O_3 and VO_x/ZrO_2 catalysts. For the VO_x/MgO catalyst, the Brønsted acid site is unlikely formed because of the strong base site present on the MgO support. Deng and co-workers [54,55] considered that the bridging –Mo–OH–Zr–, –W–OH–Zr– and –Mo–OH–Sn– groups were responsible for the strong Brønsted acid sites generated in the MoO_x/ZrO_2, WO_x/ZrO_2 and MoO_x/SnO_2 solid acids, respectively. In our case, it is likely that the strong Brønsted acid sites on the VO_x/Al_2O_3 and VO_x/ZrO_2 catalysts are also generated by the bridging –V–OH–Al– and –V–OH–Zr– groups.

In order to detect the Lewis acid site on the catalysts, we recorded ^{31}P single-pulse MAS NMR spectra of TMPO adsorbed on the three samples. As shown in Fig. 6a, only one resonance at 43 ppm is observed in the ^{31}P NMR spectrum of TMPO adsorbed on the VO_x/MgO catalyst, and this signal can be ascribed to physisorbed TMPO [33]. The adsorption of TMPO onto the VO_x/ZrO_2 catalyst produces a very broad hump of ^{31}P signal (Fig. 6b). By spectral deconvolution, three signals at 47, 58 and 68 ppm can be found. The signal at 47 ppm is due to physisorbed TMPO [56], while the other two signals at 58 and 68 ppm can be assigned to TMPO adsorbed on the weakly acidic ZrOH groups and the Brønsted acid sites, respectively. For the VO_x/Al_2O_3 catalyst (Fig. 6c), three ^{31}P NMR signals are observed at 43, 55 and 69 ppm. Similar assignment can be

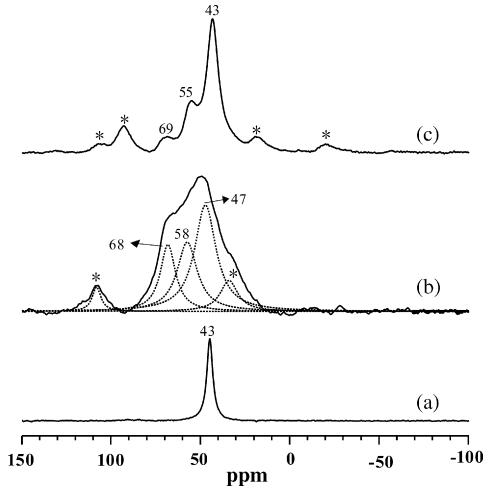

Fig. 6. ^{31}P single-pulse MAS NMR spectra (with proton decoupling) of TMPO adsorbed on (a) VO_x/MgO, (b) VO_x/ZrO_2 and (c) VO_x/Al_2O_3. The asterisk denotes spinning sidebands.

made with the former being assigned to physisorbed TMPO and the later two to TMPO adsorbed on the weakly acidic AlOH groups and the Brønsted acid sites, respectively. Based on our TMPO experimental results, we can conclude that the concentration of Lewis acid site on the catalysts is too low to be detected by NMR. Therefore, the role of Lewis acidity in the catalytic reaction can be neglected.

The quantum chemical calculation method was used to predict the acidic strength of the bridging hydroxyl groups in our proposed models containing V=O, V–O–V and V–O–Al (or Zr) bonds. The existence of these bonds was confirmed by UV and visible Raman spectroscopies [16]. The optimized structures of acetone adsorbed on the bridging Brønsted acid sites of the VO_x/Al_2O_3 and VO_x/ZrO_2 catalysts are shown in Fig. 7. Generally, the stronger the Brønsted acidity, the stronger the hydrogen bond between the carbonyl oxygen and acidic proton, resulting in a longer C=O bond length. In the complex structures, the bridging acidic O–H bond lengths are 1.060 and 1.024 Å for acetone adsorbed on the bridging –V–OH–Al– and –V–OH–Zr– groups, respectively, and the distances between the acidic proton and carbonyl oxygen are 1.463 and 1.590 Å, respectively. Meanwhile, the C=O bond lengths increase from 1.220 Å (in free gas state) to 1.238 and 1.231 Å for acetone adsorbed on the bridging –V–OH–Al– and –V–OH–Zr– groups, respectively. The larger extent of elongation of the C=O and the bridging O–H bond lengths in the adsorption complex on the VO_x/Al_2O_3 catalyst suggests that its acidic strength is stronger than that of VO_x/ZrO_2 catalyst.

Table 3
Experimental and calculated ^{13}C chemical shifts of the carbonyl carbon of acetone adsorbed on the bridging Brønsted acid sites of different proposed models

Catalyst	Acid site	^{13}C chemical shift (ppm) of acetone adsorption complex	
		Calculated	Experimental
VO_x/Al_2O_3	–V–OH–Al–	225.9	225
VO_x/ZrO_2	–V–OH–Zr–	220.8	223

The ^{13}C isotropic chemical shifts of the carbonyl carbon for acetone on the bridging Brønsted acid sites were calculated, and the corresponding results are listed in Table 3. The calculated ^{13}C chemical shifts are 225.9 and 220.8 ppm for acetone adsorbed on the acid sites of the VO_x/Al_2O_3 and VO_x/ZrO_2 catalysts, respectively, again indicative of the much stronger acid strength of the VO_x/Al_2O_3 catalyst. Since the calculated ^{13}C chemical shifts are very close to the experimentally measured values (225 and 223 ppm, respectively), we believe that our proposed models can represent the structures of Brønsted acid sites formed on the catalysts after the introduction of vanadium species onto γ-Al_2O_3 and ZrO_2 supports.

It is known that the VO_x active content is very important to the oxidation performance of VO_x-supported catalyst [16]. In the present case, the supports actually exhibit a significant effect on the product distribution of the methanol oxidation reaction. The stronger acid sites on the VO_x/Al_2O_3 catalyst surfaces direct almost the same selectivities for DMM, paraformaldehyde and formic acid, while paraformaldehyde is preferentially formed on the VO_x/ZrO_2 catalyst with less stronger acid sites

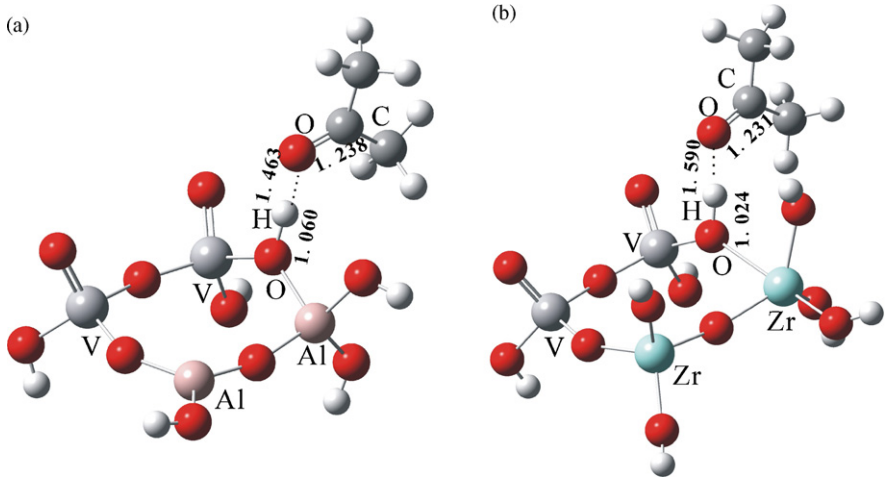

Fig. 7. Optimized structures of acetone adsorbed on the bridging Brønsted acid sites present on the catalysts: (a) VO_x/Al_2O_3 and (b) VO_x/ZrO_2. Selected bond lengths (Å) are indicated.

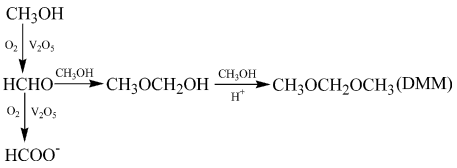

Scheme 2. Proposed pathways for methanol oxidation reaction over the catalysts [57].

and the VO_x/MgO catalyst with the base support shows high selectivity for formate. Iglesia and co-worker [57] concluded that CH_3OH converts to DMM via primary CH_3OH oxidation reactions to form HCHO and subsequent secondary reactions of HCHO with CH_3OH in steps requiring both redox and Brønsted acid sites. Brønsted acid sites are mainly involved in the formation of DMM from formaldehyde and CH_3OH (Scheme 2). Our experimental results revealed that the main products are varied from DMM, paraformaldehyde and formic acid on VO_x/Al_2O_3 to paraformaldehyde on VO_x/ZrO_2 and to formate on VO_x/MgO as the acid strength of these catalysts decreases, which is consistent with Iglesia's findings. Therefore, different acidic nature of the supports may lead to very different catalytic activities.

4. Conclusions

In summary, methanol catalytic oxidation over VO_x/Al_2O_3, VO_x/ZrO_2 and VO_x/MgO have been studied by solid-state NMR spectroscopy. Our NMR experimental and theoretical calculation results indicate that the supports have a great effect on the product distribution of methanol oxidation reaction over the supported vanadium oxide. Stronger acid sites in VO_x/Al_2O_3 lead to almost the same selectivities for dimethoxymethane (DMM), paraformaldehyde and formic acid, while weaker acid sites in VO_x/ZrO_2 favor paraformaldehyde synthesis. Furthermore, the VO_x/MgO catalyst with the base support exhibits high selectivity for formate. We also found that the interaction of VO_x and supports (γ-Al_2O_3, ZrO_2) leads to the formation of new Brønsted acid site on the VO_x/Al_2O_3 and VO_x/ZrO_2 catalysts with acidic strength much stronger than that of the acid sites originally present on the supports. Our 2-^{13}C-acetone NMR experimental reveals that the acid strength of bridging Brønsted acid sites on the VO_x/Al_2O_3 are stronger than that of VO_x/ZrO_2 catalyst which has the acid strength similar to zeolite HZSM-5. The quantum chemical calculation results of acetone adsorbed on the bridging Brønsted acid sites are in good agreement with our experimental observations.

Acknowledgment

We are very grateful to the support of the National Natural Science Foundation of China (20425311, 20573133 and 20673139).

References

[1] R. Mallinski, M. Akimoto, E. Echigoya, J. Catal. 44 (1976) 101.
[2] D.C. Argawal, P.C. Nigam, R.D. Srivastava, J. Catal. 55 (1978) 1.
[3] F. Roozenboom, P.D. Cordingley, P.J. Gellings, J. Catal. 68 (1981) 464.
[4] A. Baiker, D. Monti, J. Catal. 91 (1985) 361.
[5] D. Monti, A. Reller, A. Baiker, J. Catal. 93 (1985) 360.
[6] T. Carlson, G.L. Griffin, J. Phys. Chem. 90 (1986) 5896.
[7] L.J. Burcham, G.T. Gao, X.T. Gao, I.E. Wachs, Top. Catal. 11 (2000) 85.
[8] B. Guido, S.E. Ahmed, F. Pio, J. Phys. Chem. 91 (1987) 5263.
[9] G. Centi, Appl. Catal. A 147 (1996) 267.
[10] I.E. Wachs, B.M. Weckhuysen, Appl. Catal. A 157 (1997) 67.
[11] A. Khodakov, B. Olthof, A. Bell, E. Iglesia, J. Catal. 181 (1999) 205.
[12] P. Concepcion, M.T. Navarro, T. Blasco, J.M. Lopez Nieto, B. Panzaechi, F. Rey, Catal. Today 96 (2004) 179.
[13] M. Banares, Catal. Today 51 (1999) 319.
[14] X. Gao, I.E. Wachs, Top. Catal. 18 (2002) 243.
[15] D. Siev Hew Sam, V. Soeven, J.C. Volta, J. Catal. 123 (1990) 417.
[16] Z. Wu, H.S. Kim, P.C. Stair, S. Rugmini, S.D. Jackson, J. Phys. Chem. B 109 (2005) 2793.
[17] G.V. Isaguliants, I.P. Belomestnykh, Catal. Today 100 (2005) 441.
[18] J.L. Bars, A. Auroux, M. Forissier, J.C. Vedrine, J. Catal. 162 (1996) 250.
[19] M.W. Anderson, J. Klinowski, Nature 339 (1989) 200.
[20] N.D. Lazo, D.K. Murray, M.L. Kieke, J.F. Haw, J. Am. Chem. Soc. 114 (1992) 8552.
[21] M. Hunger, J. Weitkamp, Angew. Chem., Int. Ed. 40 (2001) 2955.
[22] A.G. Stepanov, S.S. Arzumanov, M.V. Luzgin, H. Ernst, D. Freude, J. Catal. 229 (2005) 243.
[23] B. Arstad, S. Kolboe, J. Am. Chem. Soc. 123 (2001) 8137.
[24] W.P. Rothwell, W.X. Shen, J.H. Lunsford, J. Am. Chem. Soc. 106 (1984) 2452.
[25] E.F. Rackiewicz, A.W. Peters, R.F. Wormsbecher, K.J. Sutovich, K.T. Mueller, J. Phys. Chem. B 102 (1998) 2890.
[26] A.I. Biaglow, R.J. Gorte, G.T. Kokotailo, D. White, J. Catal. 148 (1994) 779.
[27] J.F. Haw, J.B. Nicholas, T. Xu, L.W. Beck, D.B. Ferguson, Acc. Chem. Res. 29 (1996) 259.
[28] G.E. Maciel, J.F. Haw, I.S. Chuang, B.L. Hawkins, T.A. Early, D.R. Mckay, L. Petrakis, J. Am. Chem. Soc. 105 (1983) 5529.
[29] J.F. Haw, S. Chuang, B.L. Hawkins, G.E. Maciel, J. Am. Chem. Soc. 105 (1983) 7206.
[30] M. Hunger, Solid State Nucl. Magnet. Reson. 6 (1996) 1.
[31] J. Yang, M.J. Janik, D. Ma, A. Zheng, M. Zhang, M. Neurock, R.J. Davis, C. Ye, F. Deng, J. Am. Chem. Soc. 127 (2005) 18274.
[32] Q. Luo, F. Deng, Z. Yuan, J. Yang, M. Zhang, Y. Yue, C. Ye, J. Phys. Chem. B 107 (2003) 2435.
[33] Q. Zhao, W.H. Chen, S.J. Huang, Y.C. Wu, H.K. Lee, S.B. Liu, J. Phys. Chem. B 106 (2002) 4462.
[34] J.G. Fripiat, P. Galet, J. Delhalle, J.M. Andre, J.B. Nagy, E.G. Derouane, J. Phys. Chem. 89 (1985) 1932.
[35] P.J. Omalley, J. Dwyer, Zeolite 8 (1988) 317.
[36] J. Zhang, J.B. Nicholas, J.F. Haw, Angew. Chem., Int. Ed. 39 (2000) 3302.
[37] J.O. Ehresmann, W. Wang, B. Herreros, D.P. Luigi, T.N. Venkatraman, W. Song, J.B. Nicholas, J.F. Haw, J. Am. Chem. Soc. 124 (2002) 10868.
[38] J.F. Haw, T. Xu, J.B. Nicholas, P.W. Gorgune, Nature 389 (1997) 832.
[39] T. Xu, N. Kob, R.S. Drago, J.B. Nicholas, J.F. Haw, J. Am. Chem. Soc. 119 (1997) 12231.
[40] A.M. Zheng, L. Chen, J. Yang, Y. Yue, C.H. Ye, X. Lu, F. Deng, J. Chem. Soc., Chem. Commun. (2005) 2474.
[41] H. Liu, P. Cheung, E. Iglesia, J. Phys. Chem. B 107 (2003) 4118.
[42] ADF, 2004, SCM, Theoretical Chemistry, Vrije Universiteit, Amsterdam, 2004, http://www.scm.com.
[43] A.D. Becke, Phys. Rev. A 38 (1988) 3098.
[44] J.P. Perdew, J.A. Chevary, S.H. Vosko, K.A. Jackson, M.R. Pederson, D.J. Singh, C. Fiolhais, Phys. Rev. B 46 (1992) 6671.
[45] E. van Lenthe, E.J. Baerends, J.G. Snijders, J. Chem. Phys. 99 (1993) 4597.
[46] K. Wolinski, J.F. Hinton, P. Pulay, J. Am. Chem. Soc. 112 (1990) 8251.
[47] C.A. Steinbeck, B.F. Chmelka, J. Am. Chem. Soc. 127 (2005) 11624.
[48] W.W. Simons, Sadtler Carbon-13 Nuclear Magnetic Resonance Spectra, 9, Sadtler Research Laboratories, Division of Bio-Rad Laboratories Inc., 3316 Spring Garden Street, Philadelphia, Pennsylvania 19104, USA, 1982, Sample No. 1670C.

[49] S. Pilkenton, S.J. Hwang, D. Raftery, J. Phys. Chem. B 103 (1999) 11152.
[50] L.K. Carlson, P.K. Isbester, E.J. Munson, Solid State Nucl. Magnet. Reson. 16 (2000) 93.
[51] A. Philippou, M.W. Anderson, J. Am. Chem. Soc. 116 (1994) 5774.
[52] T. Xu, E.J. Munson, J.F. Haw, J. Am. Chem. Soc. 116 (1994) 1962.
[53] T. Riemer, D. Spielbauer, M. Hunger, G.A.H. Mekhemer, H. Knözinger, J. Chem. Soc., Chem. Commun. (1994) 1181.
[54] J. Xu, A. Zheng, J. Yang, Y. Su, J. Wang, D. Zeng, M. Zhang, C. Ye, F. Deng, J. Phys. Chem. B 110 (2006) 10662.
[55] J. Wang, Y. Su, J. Xu, C. Ye, F. Deng, Phys. Chem. Chem. Phys. 8 (2006) 2378.
[56] E.F. Rakiewicz, A.W. Peters, R.F. Wormsbecher, J. Phys. Chem. B 102 (1998) 2890.
[57] H. Liu, E. Iglesia, J. Phys. Chem. B 107 (2003) 10840.